

wave functions, the Compton-profile anisotropy would be independent of overlap while the form factor would have a linear dependence on the Fourier transform of the overlap term. Thus the ratio of the anisotropic term

in the form factor to that in the Compton profile would be the same as in our linear combination of atomic orbitals approach.

¹⁹C. A. Coulson, Proc. Camb. Phil. Soc. **37**, 55 (1941).

Evidence for a Surface-State Exciton on GaAs(110)*

G. J. Lapeyre and J. Anderson

Montana State University, Bozeman, Montana 59715

(Received 10 March 1975)

Synchrotron-radiation photoemission data are obtained from GaAs($\bar{1}\bar{1}0$) and (110) faces for *s* and *p* polarization which show an enhancement of valence-electron emission for initial states at and below the valence-band maximum when the photon energy is scanned through the threshold for Ga-3*d*-core to intrinsic-surface-state excitations. The enhancement is interpreted as a core surface exciton associated with the Ga dangling bonds.

The use of photoemission spectroscopy to investigate properties of occupied surface states has been extended recently to the study of empty surface states. Eastman and Freeouf have reported such unoccupied states just below the bottom of the conduction-band minimum in both Ge and GaAs.^{1,2} We have performed more extensive photoemission measurements on Zn-doped *p*-type GaAs which indicate that the excitations observed by Eastman and Freeouf are not surface states in the conventional sense, but are more properly thought of as "surface excitons." We believe that these results represent the first identification of surface excitons.

The photoemission techniques used here exploit both the continuum nature and strong polarization of the synchrotron radiation from the storage ring at the University of Wisconsin Physical Sciences Laboratory.³ Rather than measure the energy distribution curve (EDC) of photoemitted electrons we measure what we call the constant initial-energy spectrum (CIS). This is done by monitoring the electron counting rate as the photon energy $h\nu$ and kinetic-energy window E_f of our analyzer are swept synchronously so that $h\nu - E_f = -E_i$ remains constant, where E_i is the initial-state energy. An alternate mode of operation which we refer to as the constant final-energy spectrum (CFS) is obtained by sweeping $h\nu$ while keeping E_f constant. The "partial-yield" curves reported in Ref. 1 are CFS's in our terminology.² Descriptions of the CIS and CFS modes have been reported elsewhere.^{4,5} To probe the properties of the empty surface states, one has to detect the photoemissive contribution

which results from core to surface-state excitations through the intermediary of a decay process.^{1,4} As discussed below, measurement of CIS's rather than CFS's permits one to distinguish between two alternative decay processes for photoexcited electrons. Further, CIS data are obtained for each of the four cases where the polarization \hat{E} is perpendicular or nearly parallel to the Ga dangling bond or the As dangling bond.

The transitions at issue in these experimental studies are those that occur at the threshold for excitation of the Ga-3*d*-core states lying 18.7 ($d_{5/2}$) and 19.2 ($d_{3/2}$) eV below the valence-band maximum, which is chosen for the energy zero. The latter binding energies are obtained from EDC and CFS data and are consistent with those in the literature.¹ The narrow pair of peaks found near 20 eV in the CIS's of Fig. 1 are attributed to an enhanced emission level occurring at the core threshold. The doublets are split by the core-spin-orbit splitting.¹ The structures occurring at lower energies are due to valence-electron excitations and are shown for the purpose of establishing a reference level for the strength of the enhancement doublets. The term valence electron is used instead of valence band because valence surface states probably contribute to the emission⁶; however, their properties do not directly bear on the issue. Each spectrum in Fig. 1 is obtained for different polarization and/or crystal orientations but the same $E_i = -1.2$ eV; E_i is a parameter for CIS's. For the upper curve in Fig. 1—($\bar{1}\bar{1}0$) face and *p* polarization—the doublet occurs at 19.65 and 20.15 eV

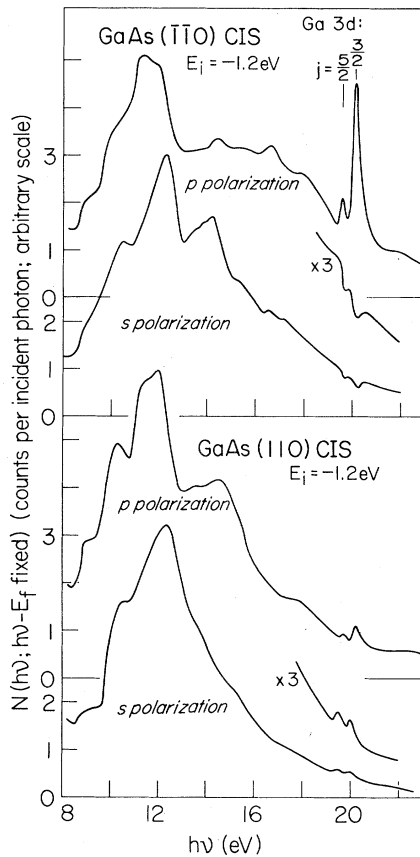


FIG. 1. Constant initial-energy spectra (CIS's) for four polarization and/or crystal orientations which are described in the text. The Ga-3d-core enhancement is noted.

with full widths at half maximum (FWHM) of 0.21 ($d_{5/2}$) and 0.26 ($d_{3/2}$) eV for a monochromator band pass $\Delta h\nu = 0.13$ eV. We agree with the conclusion of EF¹ that the phenomenon is a surface effect and find that a light overlayer of Sb eliminates the doublet while the EDC's remain approximately unchanged.

To present the consequences of the doublet observed in the CIS's we note the following properties: (1) The $h\nu$ values for the doublets are independent of E_i ; (2) the doublet occurs for all E_i 's, even those arbitrarily close to the valence-band maximum; (3) the $h\nu$ values are less than the energy differences between the cores and the conduction-band minimum. We refer to these peaks as enhancements of the valence emission since the energies of the emitted electrons are much greater than direct core excitations. These properties are most easily deduced from CIS's rather than CFS's or EDC's because the back-

ground emission exhibits minimal modulations. Because this is not direct emission, in the above sense, it is due to some decay process. Two such processes have been presented in the literature^{4,7}; one is the Auger decay and the other is direct recombination (DR), both occurring via a configuration interaction. The two processes can be differentiated because they excite electrons with different final energies. The Auger decay comes about by a valence electron filling the core hole with another valence excitation absorbing a like quantity of energy for energy conservation. The maximum final energy for the Auger process is *smaller than* that for electrons excited from the valence-band maximum by the difference between the photon energy at enhancement and the core-binding energy⁴; Auger electrons cannot appear in the CIS's for values of $|E_i| < 0.95$ eV. The enhanced electrons do, however, appear at all energies above the Auger limit so Auger decay cannot account for all of the enhancements. Thus the enhanced emission above the limit is attributed to a direct-recombination process, where the core hole and the electron recombine with a transfer of energy to valence excitations. In the DR process the initial hole-electron pair needs to be very localized. Such a localization points to the inadequacy of the usual density-of-states band picture and strongly suggests the presence of exciton binding for the hole-electron pair.

Identification of the DR process also follows from an examination of the energy distribution for the enhanced emission. For (110) surface in *p* polarization the enhancement is strong enough to be seen in the EDC shown in Fig. 2 (solid line), taken at a photon energy near maximum enhancement, as compared with EDC's taken at closely neighboring energies above and below the resonance maximum. The emission distribution due to the DR decay may be approximated by the valence electron density of states if effects due to matrix-element variations, scattering, etc. are ignored.⁸ As observed in the $h\nu = 20.2$ eV EDC the enhanced distribution for $-4.5 < E_i < 0$ eV follows closely the emission when $h\nu$ is off resonance in agreement with the above approximation. The possibility of significant Auger-decay enhancement at the latter energies is discounted on the grounds that in such a case the enhancement distribution should resemble the self-convolution of the density of states. A self-convolution, calculated from the theoretical bulk density of states of Eastman *et al.*,⁹ is shown in the lower part of

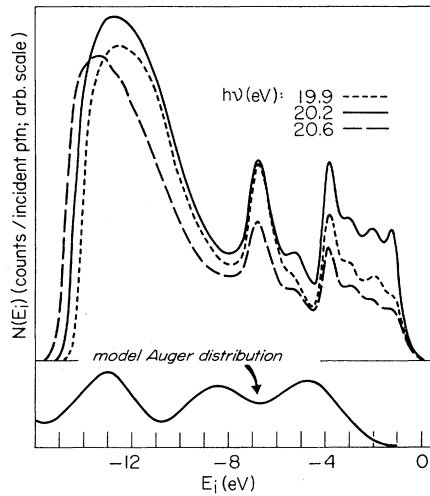


FIG. 2. EDC's for the $(\bar{1}\bar{1}0)$ surface in p polarization. The model Auger distribution is plotted against initial energy E_i for $h\nu = 20.2$ eV.

Fig. 2. Clearly the Auger process can not account for the majority of the enhanced emission for $-4.5 < E_i < 0$ eV.

The polarization dependence of the exciton enhancement is exemplified in the data of Fig. 1 which contain four different geometries. The exciton emission is dramatically larger for the case labeled $(\bar{1}\bar{1}0)$ p polarization in Fig. 1 where the \hat{E} vector has its largest component parallel to the Ga dangling bond (DB).¹⁰ In the other three geometries \hat{E} is either perpendicular to the Ga DB or nearly so. It is this observation that leads us to believe that the phenomenon under examination is associated with the Ga DB.

The four geometric configurations used for data collection are summarized by the schematic in Fig. 3; the specific case shown is for s -polarization-induced emission from the $(\bar{1}\bar{1}0)$ face. The s -to- p polarization change is made by rotating the crystal by 90° *in situ*.¹⁰ The rotation axis is common to the axis of the cocylindrical-mirror electron energy analyzer (CMA) which means that the CMA collection cone remains unchanged during the rotation. The crystal is oriented—as shown in Fig. 3—(1) so the Ga DB (open arrow) rotates during crystal rotation, and (2) so the As DB (solid arrow) is approximately static during rotation. The latter approximation comes about because the $[\bar{1}\bar{1}1]$ direction makes a 7° angle with the CMA axis. Thus two of the four geometries are obtained by changing the polarization. The remaining two geometries are obtained when the

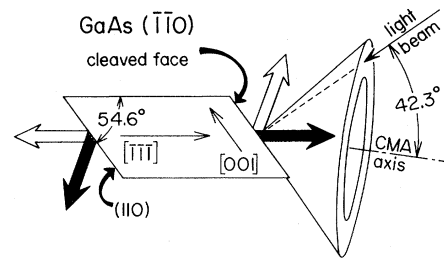


FIG. 3. Schematic for the crystal, light beam, and CMA geometry. The s -polarization case is shown since \hat{E} is perpendicular to the page. The light beam is normal to the $(\bar{1}\bar{1}0)$ face. The Ga dangling bond (open arrow), As dangling bond (solid arrow), indicated crystal directions, light beam, and CMA axis all lie in the page.

Ga DB and As DB are interchanged by turning the crystal end for end, remounting, and then cleaving *in situ* for the (110) face. The (111) and $(\bar{1}\bar{1}\bar{1})$ faces are determined by their etch properties.¹¹ Thus, for the (110) cleave, it is the As DB which is perpendicular to \hat{E} in s polarization and nearly parallel to \hat{E} in p polarization; the exciton enhancement is weak with approximately the same strength in *both* cases.

While the existence of the DR emission doublets is strong direct evidence for an excitonic model, the model can account for several remarkable properties exhibited by the doublets which are difficult to account for with a density-of-states model. First, one notes that the intensities of the $j = \frac{5}{2}$ and $\frac{3}{2}$ components are reversed from the 6:4 statistical weight for the core states. Such an intensity reversal has been explained by the theoretical work of Onodera and Toyozawa¹² which shows that the exciton oscillator strength is strongly dependent on exchange. Second, the relative amplitudes of the two peaks in the doublets as well as the $h\nu$ values for the doublets depend on the polarization/crystal orientation. For example, (1) just rotating the (110) face from the s to p polarization (see the lower pair of curves in Fig. 2) the peaks shift from 19.5 and 20.0 eV to 19.7 and 20.2 eV—the shift is approximately equal to the FWHM; (2) the doublet in the $(\bar{1}\bar{1}0)$ s -polarization CIS are minimums instead of peaks; and (3) the strength of the reversal is dependent on the polarization and/or crystal orientation. The doublet separation is the same for all orientations. These observations might be explained in terms of the Fano effect.¹³ The exciton, a bound excitation, is degenerate with the valence-excitation continuum so that the total

wave function contains bound and continuum terms. Thus the expression for the transition rate contains cross terms in addition to the exciton and the interband direct terms. The interband term describes the emission level in the CIS's under the exciton doublet. The cross terms, which may be called interference terms, can be negative and their maximum strength does not have to occur at the same $h\nu$ value as that for the exciton term. One would expect the interference terms to be weak; however when the exciton is polarization "forbidden" the magnitudes of the direct and interference terms could be comparable. Thus, the combination of the exciton and interference terms could give peaks differing in position and amplitude as observed in the data. Further, the narrow width of the enhancement lines is more consistent with an exciton model than a density-of-states model.

In conclusion we have presented a number of observed properties for the photoemission enhancement at the core to surface-state edge and suggested how they all may be understood with an excitonic model. Our results suggest that the exciton is small; that is, the Frenkel picture is more appropriate than the Wannier picture.

We acknowledge many detailed discussions with J. Hermanson and valuable comments by N. Smith and D. Eastman. The technical support at Montana State University and the Synchrotron Center was essential.

*Research sponsored by the U. S. Air Force Office at Scientific Research, Air Force Systems Command, under Grant No. AFOSR-71-2061. The storage ring is supported by the National Science Foundation Grant No. 144-F805.

¹D. E. Eastman and J. L. Freeouf, Phys. Rev. Lett. **33**, 1601 (1974).

²The GaAs CFS data obtained during these experiments are consistent with those in Ref. 1.

³The spectral radiation, dispersed by a normal-incidence monochromator, is determined with sodium salicylate fluorescence. The properties of the optical system are used to estimate an 88% polarization purity.

⁴G. J. Lapeyre *et al.*, Solid State Commun. **15**, 1601 (1974).

⁵G. J. Lapeyre *et al.*, Phys. Rev. Lett. **33**, 1290 (1974).

⁶J. E. Rowe and H. Ibach, Phys. Rev. Lett. **32**, 421 (1974).

⁷R. Haensel *et al.*, Phys. Rev. Lett. **23**, 530 (1969); G. W. Rubloff, Phys. Rev. B **5**, 662 (1972).

⁸The additional peak near -1.1 eV in the $h\nu=20.2$ -eV EDC is probably due to DR-enhanced emission from the occupied surface states. Discussion of this point is beyond the scope of this paper.

⁹D. E. Eastman *et al.*, Phys. Rev. B **9**, 3473 (1974). Figure 4 in this paper shows the behavior of strong Auger enhancement in a Ge EDC.

¹⁰While "s polarization" is literal the term "p polarization" is used for convenience since a small s component remains after the 90° rotation.

¹¹O. W. Ranke and K. Jacobi, Solid State Commun. **13**, 705 (1973).

¹²Y. Onodera and Y. Toyozawa, J. Phys. Soc. Jpn. **22**, 833 (1967).

¹³U. Fano, Phys. Rev. **124**, 1866 (1961).

New Mechanism for a Charge-Density-Wave Instability

T. M. Rice* and G. K. Scott

Department of Physics, Simon Fraser University, Burnaby, British Columbia, Canada V5A 1S6

(Received 20 March 1975)

It is shown that a two-dimensional energy band with saddle points at the Fermi energy is unstable against charge density wave formation. The distorted phase is metallic with only a relatively small area of Fermi surface truncated at the saddle points. It is suggested that this model applies to the layer compounds $2H$ -TaSe₂, $2H$ -TaS₂, $2H$ -NbSe₂, and $4Hb$ -TaS₂.

Lomer¹ first pointed out that a band structure in which electron and hole surfaces "nest" can favor the formation of a superlattice instability.² In this Letter we show that in a two-dimensional band structure a superlattice instability can arise in a model which does not have "nesting" in the usual sense. In this model large areas of Fermi

surface are not truncated and indeed the low-temperature state may well be a better metal than the high-temperature phase. We suggest that this model applies to the $2H$ -polytype layer compounds where charge-density waves (CDW) have recently been discovered.³⁻⁷ There is a striking contrast between the effects of the CDW transition on the